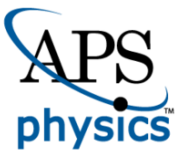

Anomalous Quantum Hall Effect of Light in Bloch-Wave Modulated Photonic Crystals

Kejie Fang and Yunkai Wang

Phys. Rev. Lett. **122**, 233904 — Published 14 June 2019

DOI: 10.1103/PhysRevLett.122.233904

Anomalous quantum Hall effect of light in Bloch-wave modulated photonic crystals

Kejie Fang[1, 2, *] and Yunkai Wang[2, 3]

[1] *Department of Electrical and Computer Engineering, University of Illinois at Urbana-Champaign, Urbana, IL 61801 USA*

[2] *Micro and Nanotechnology Laboratory, University of Illinois at Urbana-Champaign, Urbana, IL 61801 USA*

[3] *Department of Physics, University of Illinois at Urbana-Champaign, Urbana, IL 61801 USA*

Effective magnetic fields have enabled unprecedented manipulation of neutral particles including photons. In most studied cases, the effective gauge fields are defined through the phase of mode coupling between spatially discrete elements, such as optical resonators and waveguides in the case for photons. Here, in the paradigm of Bloch-wave modulated photonic crystals, we show creation of effective magnetic fields for photons in conventional dielectric continua for the first time, via Floquet band engineering. By controlling the phase and wavevector of Bloch waves, we demonstrated anomalous quantum Hall effect for light with distinct topological band features due to delocalized wave interference. Based on a cavity-free architecture, in which Bloch-wave modulations can be enhanced using guided-resonances in photonic crystals, the study here opens the door to the realization of effective magnetic fields at large scales for optical beam steering and topological light-matter phases with broken time-reversal symmetry.

Photons, being charge neutral, are not susceptible to magnetic fields. Recently, several methods have been proposed to create effective magnetic fields for photons, including chiral mode coupling [1] and dynamic index modulation [2], leading to topological photonic states [3, 4] and nonreciprocal light propagation [5, 6]. In the scheme of dynamic index modulation, the effective gauge field is equivalent to the phase of a point modulation that is exerted to mediate the coupling between two spatially localized optical resonators with different frequencies [2]. Such a revelation enables analogies between modulated optical resonator lattices and condensed matter systems under magnetic fields via commonly used tight-binding models, which nonetheless imposes challenges for experimental realization and practical uses. However, it is unknown how to create effective magnetic fields for photons in a continuum of conventional dielectrics, where electromagnetic fields are delocalized, invalidating the notion of local phase of mode coupling for effective gauge fields. Here, we study a new paradigm of dynamically modulated continua, that is photonic crystals subject to Bloch-wave modulations, in which spatial gauge fields for photons are revealed via Floquet band engineering [7, 8]. In this approach, the continuum modulation induces static-band hybridization, leading to an equation of motion for electromagnetic waves that resembles that of charged particles under magnetic fields.

The paradigm of modulated electromagnetic continuum not only extends the concept of effective magnetic fields for photons to a largely unexplored yet experimentally accessible regime, but also leads to topological photonic effects that have not been demonstrated before. As we will show, by selecting the wavevectors of Bloch-wave modulations, net effective magnetic flux through the unit cell of photonic crystals vanishes. Nevertheless, the Floquet bands can still attain nonzero Chern numbers in the presence of time-reversal symmetry breaking caused by the dynamic modulation. This result represents the first anomalous quantum Hall effect for light in Floquet engineered photonic systems.

Here, we developed a first-principle based formalism along with *ab initio* simulations to reveal unique topological band features in Bloch-wave modulated photonic crystals due to delocalized wave interference. We also propose to use guided resonances or bound states in the continuum [9, 25, 33] to enhance the strength of Bloch-wave modulations that can be readily implemented with highly-transducing optical or acoustic pump fields [12, 30]. As a result, the proposed paradigm of modulated continuum here opens the door to large-scale realization of effective magnetic fields for photons in normal dielectrics for new types of beam steering, dynamic signal processing, and topological states with broken time-reversal symmetry, that are highly tunable and reconfigurable via controlling the parameters of Bloch waves.

To study photonic crystals under continuum modulations, we start from Maxwell's equation with isotropic and temporally-periodic permittivity $\epsilon(\mathbf{r},t) = \epsilon(\mathbf{r}) + \delta(\mathbf{r},t)$:

$$i\frac{\partial}{\partial t}\begin{pmatrix}\epsilon(\mathbf{r},t)\mathbf{E}\\ \mathbf{H}\end{pmatrix} = \begin{pmatrix} & i\nabla\times\\ -i\nabla\times & \end{pmatrix}\begin{pmatrix}\mathbf{E}\\ \mathbf{H}\end{pmatrix}. \quad (1)$$

Here, $\epsilon(\mathbf{r})$ is the spatially-periodic permittivity which defines the static photonic crystal, and $\delta(\mathbf{r},t) = \delta(\mathbf{r})\cos\big(\omega t+\phi(\mathbf{r})\big)$ is the temporal modulation of the permittivity with frequency ω, amplitude $\delta(\mathbf{r})$, and phase $\phi(\mathbf{r})$, all of which are real. Note this form represents the most general monochromatic modulations. We have set $\epsilon_0 = \mu_0 = 1$ and $\mu = 1$ as for most dielectric materials at optical frequencies. Because of the time-periodicity of the permittivity, according to Floquet theorem [14], the eigenmodes of Eq. 1 can be found by decomposition of the fields into harmonics of the modulation frequency,

i.e., $(\mathbf{E} \quad \mathbf{H})^T \equiv \Psi = \sum_{n=-\infty}^{\infty} \psi_n e^{-i\chi t + in\omega t}$, where χ is the quasi-frequency [15]. We coin the resulting time-independent eigenmode equation the Floquet-Maxwell equation.

When the modulation has the form of Bloch waves, i.e., $\delta(\mathbf{r})e^{i\phi(\mathbf{r})} = u(\mathbf{r})e^{i\mathbf{q}\cdot\mathbf{r}}$ and $u(\mathbf{r})$ a periodic function (note $\phi(\mathbf{r})$ needs not to be $\mathbf{q}\cdot\mathbf{r}$), we call such modulated dielectric structures the Floquet photonic crystal. If the periodicities of $u(\mathbf{r})$ and the static photonic crystal are commensurable, then by applying a gauge transformation $U_{\text{gauge}} : \psi_n \rightarrow e^{in\mathbf{q}\cdot\mathbf{r}}\psi_n$, the Floquet-Maxwell equation becomes spatially-periodic and thus the eigenvalue χ can be labeled by a Bloch wavevector $\mathbf{k}$, forming the Floquet bandstructure [15]. According to this formalism, the generation of Floquet bandstructure, to the leading order, can be intuitively understood as the result of modulation induced static-band hybridization after frequency and momentum shift of the bands by ω and $\mathbf{q}$, respectively. Because of the non-vanishing momentum of the modulation, the Floquet bandstructure, with infinitely repeated branches (i.e., $\chi + n\omega$, $\forall n$, is also a solution of the Floquet-Maxwell equation), has the property $\chi(\mathbf{k}+\mathbf{q}) = \chi(\mathbf{k}) - \omega$.

With a spatially varying modulation phase $\phi(\mathbf{r})$, time-reversal symmetry in modulated photonic crystals is explicitly broken, as the modulated permittivity is not invariant under time reversal $t \rightarrow -t$ for arbitrary positions. We use Floquet band engineering, i.e., modulation induced static-band coupling, to derive an effective gauge field for photons. For this purpose, we consider two static bands under dynamic modulations with a frequency close to the bandgap which is larger than the bandwidth of each band. In this case, one can write down an approximate coupled-*band* equation as reminiscence of the Floquet-Maxwell equation,

$$\frac{\partial^2 \mathbf{H}_1}{\partial t^2} = -\nabla \times \frac{1}{\epsilon}\nabla \times \mathbf{H}_1 + \nabla \times \frac{\delta}{\epsilon^2} e^{i\phi} \nabla \times \mathbf{H}_2, \quad (2)$$

$$\frac{\partial^2 \mathbf{H}_2}{\partial t^2} = -\nabla \times \frac{1}{\epsilon}\nabla \times \mathbf{H}_2 + \nabla \times \frac{\delta}{\epsilon^2} e^{-i\phi} \nabla \times \mathbf{H}_1, \quad (3)$$

where $\mathbf{H}_{1,2}$ are the magnetizing fields associated with the two bands. The effective gauge field for photons can be identified by comparing the equation of motion for the electromagnetic fields of one band with the Hamiltonian of charged particles in the presence of gauge fields, i.e., $\hat{H} = (-i\nabla - q\mathbf{A})^2/2m$, where the gauge field is the imaginary coefficient of the term linear in $\nabla(\,\cdot\,)$. Using this method, we find

$$\mathbf{A}_{\text{eff}}(\mathbf{r}) = \frac{1}{\omega^2}\text{Im}\left\{\nabla \cdot \left(\frac{\delta}{\epsilon^2} e^{i\phi} \nabla (\nabla \frac{\delta}{\epsilon^2} e^{-i\phi})\right)\right\} \quad (4)$$

for transverse electric (TE) modes (the $\cdot$ means the scalar product between the first ∇ and the last ∇) and

$$\mathbf{A}_{\text{eff}}(\mathbf{r}) = \frac{2}{\omega^2}\text{Im}\left\{\nabla^2 (\frac{\delta}{\epsilon^2} e^{i\phi} \nabla \frac{\delta}{\epsilon^2} e^{-i\phi})\right\} \quad (5)$$

for transverse magnetic (TM) modes in two-dimensional photonic crystals, respectively [15].

From Eqs. 4 and 5, it is remarkable that the effective gauge field is largely determined by the modulation phase, similar to the case of discretely modulated resonator lattices [2]; it is zero if $\phi(\mathbf{r}) = \text{const.}$. However, in the continuum the effective gauge field can be defined in space by the modulation phase point-to-point, while in resonator lattices it is implicitly related to the modulation phase through a line integration. One also finds that for Bloch-wave modulations with $u(\mathbf{r})$ having the same periodicity as the static photonic crystal, $\mathbf{A}_{\text{eff}}(\mathbf{r})$ is periodic and net effective magnetic flux through a unit cell vanishes. As we will show next, for certain Floquet photonic crystals, even though the net magnetic flux is zero through a unit cell, the Floquet bands attain nonzero Chern numbers. This represents a photonic analogue of the anomalous quantum Hall effect [16], which is distinct from the photonic analogues of quantum Hall and quantum spin Hall effects proposed in Ref. [2] and Ref. [1], respectively.

The example of Floquet photonic crystal we studied begins with a two-dimensional photonic crystal with a triangular lattice (lattice constant a) of dielectric rods ($r = 0.27a$) with relative permittivity $\epsilon_r = 12$ (corresponding to silicon or gallium arsenide) in a background with relative permittivity $\epsilon_r = 2$ (corresponding to silicon dioxide) (Fig. 1a). A honeycomb sub-lattice (lattice constant $3a$) is created inside the triangular lattice, consisting of smaller rods ($r = 0.145a$, $\epsilon_r = 12$) and holes ($r = 0.27a$, $\epsilon_r = 1$). The bandstructure of the TM modes calculated using plane-wave expansion method [17] is shown in Fig. 1b and the out-of-plane electric field of the modes of the highlighted band 2 at Γ and K points is shown in Fig. 1c. As time-reversal symmetry is not broken in the static photonic crystal, all the bands are topologically trivial with zero Chern numbers.

Next we introduce temporal modulations of permittivity in order to couple bands 1 and 2 in Fig. 1b to create topologically nontrivial Floquet bands. The frequency of the modulation is slightly larger than the bandgap between the two bands and its spatial profile has the following form,

$$\delta(\mathbf{r})e^{i\phi(\mathbf{r})} = \sum_{j=1}^{3} u_j(\mathbf{r}) e^{i(\mathbf{k}_j \cdot \mathbf{r} + \phi_j)}, \quad (6)$$

where $u_{1,2,3}(\mathbf{r})$ are functions with the same spatial periodicity as the static photonic crystal and we choose the coordinate origin at the center of an air hole. The modulation of Eq. 6 is a superposition of three Bloch

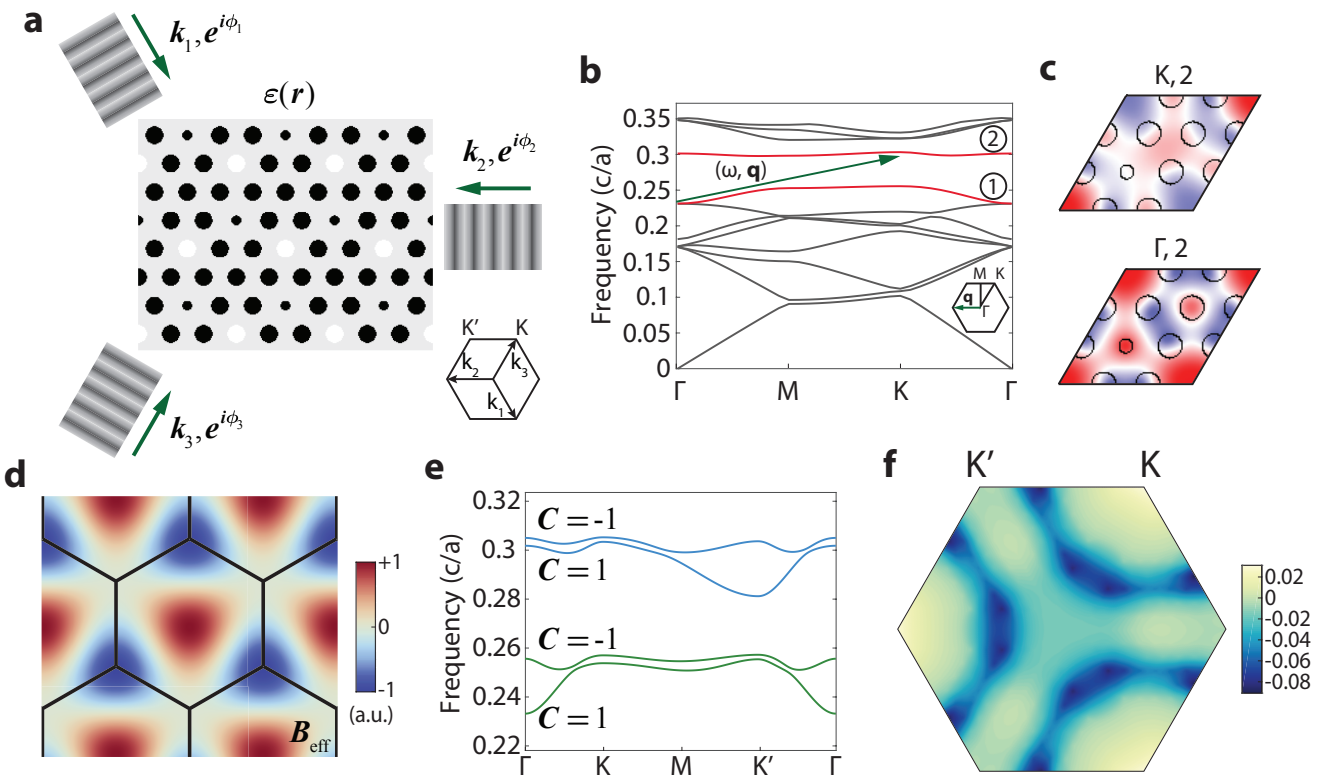

FIG. 1. **Effective magnetic fields in the Floquet photonic crystal.** **a**, The Floquet photonic crystal consists of a static photonic crystal and permittivity modulations of three Bloch waves with momenta equal to the three K points and phases $\phi_{1,2,3}$. Black, gray, and white areas in the static photonic crystal have relative permittivity 12, 2, and 1, respectively. **b**, Bandstructure of the TM modes of the static photonic crystal. The permittivity modulation with frequency ω and Bloch momentum $\mathbf{q}$ (green arrow) is used to couple the two highlighted bands (red). **c**, Out-of-plane electric field in the unit cell corresponding to the modes of band 2 at Γ and K points. **d**, Distribution of the effective magnetic field $\mathbf{B}_{\text{eff}}$ induced by the Bloch-wave modulations for $\phi_1 = 0$, $\phi_2 = 2\pi/3$, and $\phi_3 = 4\pi/3$. The net effective magnetic flux through the Wigner-Seitz unit cell is zero. **e**, Floquet bandstructure of the modulated photonic crystal, formed from the hybridization of static bands 1 and 2 of **b**. Chern number of each band is indicated for the modulation parameters specified in the text. **f**, Berry curvature in the Brillouin zone for the top blue Floquet band in **e**.

waves, which could lead to rotating distribution of permittivity. For example, if we consider the case where $\mathbf{k}_{1,2,3}$ are the three equivalent K points in the Brillouin zone, $u_{1,2,3}(\mathbf{r}) \equiv \bar{u}(\mathbf{r})$ possessing 120° rotational symmetry, and $\phi_j = \frac{2(j-1)\pi}{3}$, then we have $\hat{R}_{120^\circ}\epsilon(\mathbf{r},t) = \epsilon(\mathbf{r}, t - 2\pi/3\omega)$, where $\hat{R}_{120^\circ}$ is the operation of 120° clockwise rotation in real space. As such, by adjusting the relative phase between the Bloch-waves, we can effectively circulate the permittivity and change its chirality.

Meanwhile, because $\mathbf{k}_i - \mathbf{k}_j$ are reciprocal lattice vectors, $\delta(\mathbf{r})e^{i\phi(\mathbf{r})}$ is by itself of the Bloch-wave form, with a Bloch wavevector $\mathbf{q} = \mathbf{k}_j$, $\forall j$. The effective magnetic field for band 2 induced by the modulation is calculated using $\mathbf{B}_{\text{eff}}(\mathbf{r}) = \nabla \times \mathbf{A}_{\text{eff}}(\mathbf{r})$ and Eq. 5 for $\bar{u}(\mathbf{r}) \propto \epsilon(\mathbf{r})^2$ and $\phi_j = \frac{2(j-1)\pi}{3}$, which is shown in Fig. 1d. The net magnetic flux through the Wigner-Seitz cell is zero as expected. Fig. 1e shows the calculated TM Floquet bands (with two repeated branches) by coupling the static bands 1 and 2 with modulation parameters $\omega = 0.0491 \times 2\pi c/a$, $\phi_j = \frac{2(j-1)\pi}{3}$, and $\bar{u}(\mathbf{r}) = 0.25$ (in dielectrics) or 0 (in air). We see that K and K' points are no longer equivalent due to the momentum-carrying modulation. Although the net magnetic flux through a unit cell is zero, we find each Floquet band has nonzero Chern number $C = \pm 1$ [15], with the Berry curvature of one Floquet band shown in Fig. 1f. This result represents a photonic analogue of the anomalous quantum Hall effect [16] realized in a structure beyond tight-binding models, and indicates the existence of one-way edge modes in the Floquet bandgap [18], which are truly robust against any structural defects.

We numerically demonstrate the anomalous topological edge mode through finite-difference time-domain (FDTD) simulation using Maxwell's equation. The full simulation domain is shown in Fig. 2a with $a = 0.37$ μm. The boundaries of the simulation domain are composed of perfectly-matched layers. The Floquet photonic

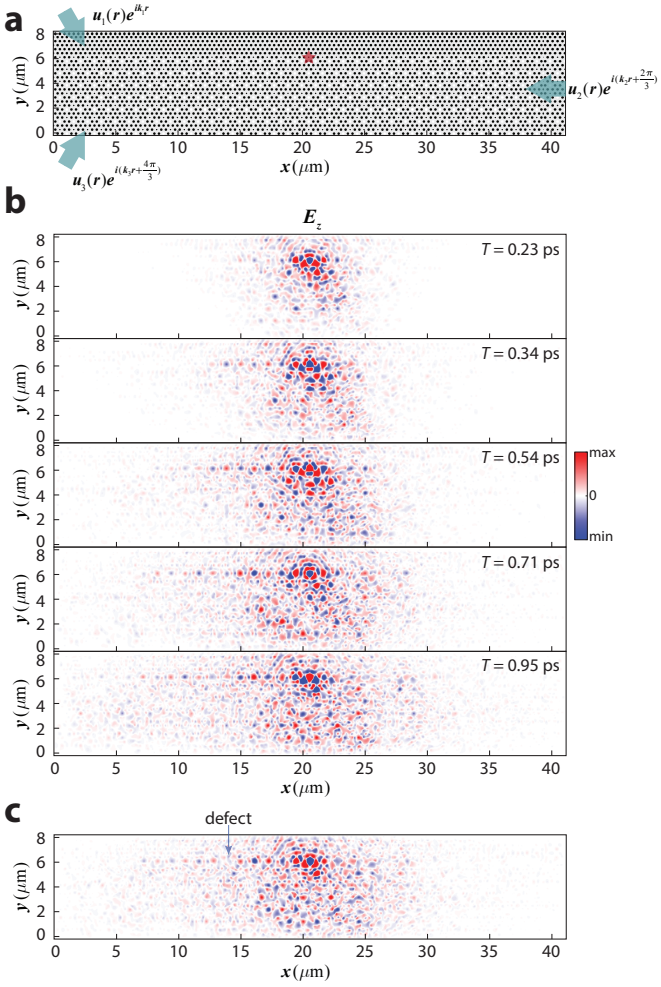

FIG. 2. **The anomalous topological edge mode. a**, The full photonic structure used in the FDTD simulation with three Bloch-wave modulations with phase lagging of $2\pi/3$. The star indicates the location of the point source. **b**, Propagation of the electric field E_z excited by the TM-polarized continuous-wave point source. A left-propagating one-way mode exists on the edge ($y \sim 6$ μm) of the Floquet photonic crystal. **c**, Reflection-immunity of the one-way edge mode in the presence of a defect. Here the defect is created by removing a small dielectric rod on the edge.

crystal occupies part of the simulation domain with an edge at $y \sim 6$ μm. The applied temporal modulation is the same as that used for the calculation of Floquet bandstructure above. A TM-polarized, continuous-wave point source with frequency $\omega_s/2\pi = 0.2549c/a = 206.7$ THz on the edge of the Floquet photonic crystal is used to excite the electromagnetic waves. Time-evolution of the excited electric field is shown in Fig. 2b, where a one-way edge mode can be clearly identified, along with bulk excitations due to the incomplete Floquet bandgap, which can be optimized by further engineering of the photonic crystal and temporal modulation. When the edge mode encounters a defect, it keeps unidirectional propagation without reflection (Fig. 2c), which is the evidence of topological protection. Note the appearance of one-way edge mode after the defect is not due to the re-excitation by bulk fields, because of its phase coherence, while the bulk fields have fluctuating phase distribution along the edge.

The topological properties of Floquet photonic crystals can be controlled by the phase of Bloch waves, which also determines the distribution of the effective magnetic field in real space. Fig. 3a shows a phase diagram of the model above, where topologically different phases with Chern number ranging from 0 to -2 exist. The distribution of the effective magnetic field in the Wigner-Seitz cell for a few phases is shown in Fig. 3b. In contrary to the tight-binding model of anomalous quantum Hall effect [16], where the sign of Chern number is related to the chirality of electron hopping amplitude, the sign of Chern number in this continuum model is not directly related to the chirality of modulations, i.e., $\phi_3 > \phi_2 > \phi_1$ or $\phi_2 > \phi_3 > \phi_1$, and the two chiralities have very different Chern number distributions. We also find that if the modulation strength is increased, positive Chern number appears around $\phi_1 = \phi_2 = \phi_3 = 0 \bmod 2\pi$ [15], which is remarkable as intuitively the Chern number is expected to be zero when the chirality of modulation is absent. These novel topological band features in Floquet photonic crystals are largely due to the delocalized wave interference in the continuum and difficult to produce in tight-binding type of systems.

Using Bloch-wave modulations to realize dynamic beam steering and topological photonic states whose property can be reconfigured by controlling the phase and wavevector of Bloch waves has practical significance. Bloch waves are eigenmodes of periodic structures and can be naturally excited by pumps with the frequency and wavevector that satisfy the dispersion relation. When multiple Bloch waves are used, the relative phases can be controlled by continuously tunable phase shifters. Such Bloch-wave induced permittivity modulations can be generated through nonlinear optical effects or optomechanical interactions with optical and acoustic traveling waves, respectively. By trapping the optical or acoustic pump waves in guided resonances of photonic crystals [9, 25, 33], one can significantly enhance the modulation strength in a large area with experimentally available pump power [15]. While in this paper we considered modulation induced inter-band coupling, low-frequency mechanical modulations are more suitable for intra-band coupling which might also result in non-trivial Floquet bands.

In summary, we have revealed the generation of effective magnetic fields for photons in photonic crystals under continuous spatio-temporal modulations. In this paradigm, we showed a photonic analogue of anomalous quantum Hall effect with unique topological band fea-

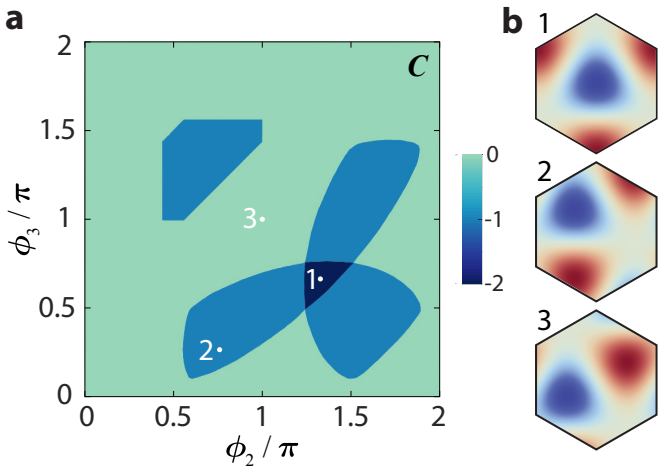

FIG. 3. **Phase diagram of the Floquet photonic crystal.** **a**, The Chern number of the higher frequency band of the Floquet two-band model for varying ϕ_2 and ϕ_3 ($\phi_1 = 0$). **b**, The effective magnetic field in the Wigner-Seitz cell corresponding to the phases indicated by points 1 $(4\pi/3, 2\pi/3)$, 2 $(3\pi/4, \pi/4)$, and 3 (π, π). Fig. 1d corresponds to point $(2\pi/3, 4\pi/3)$. For the calculation of the effective magnetic field, we used $\bar{u}(\mathbf{r}) \propto \epsilon(\mathbf{r})^2$ to remove the higher order texture due to the static permittivity distribution in the photonic crystal.

tures due to delocalized wave interference. Other than that, a variety of combinations of spatio-temporal modulations and static photonic crystals can be explored to implement physics that otherwise seems difficult with discretely-modulated resonator lattices, including those models requiring nonreciprocal phase on beyond-nearest-neighbor couplings. For instance, the scenario when the modulations have different periodicity than that of the static photonic crystals, e.g., when $\mathbf{k}_i - \mathbf{k}_j$ in Eq. 6 are not the primitive reciprocal lattice vectors, might be used to generate fractal photonic spectra, such as the Hofstadter butterfly [19]. Beam steering using effective gauge fields [6, 20] becomes feasible in the continuum case, as it avoids the mode matching issue between single-mode beams and arrays of resonators which discretely sample the beam. One could also use the modulated continuum to realize "light stopping" [21]. To that end, modulations with $\mathbf{q} = 0$ should be used in order to preserve the wavevector components of the signal pulse; then by adiabatically tuning the modulation amplitude, the topography of the coupled Floquet bands alters, e.g., shift of band edges, causing substantial change of the group velocity of light for coherent information storage.

* kfang3@illinois.edu

[1] Hafezi, M., Demler, E. A., Lukin, M. D. & Taylor, J. M. Robust optical delay lines with topological protection. *Nature Physics* **7**, 907 (2011).
[2] Fang, K., Yu, Z. & Fan, S. Realizing effective magnetic field for photons by controlling the phase of dynamic modulation. *Nature Photonics* **6**, 782 (2012).
[3] Hafezi, M., Mittal, S., Fan, J., Migdall, A. & Taylor, J. Imaging topological edge states in silicon photonics. *Nature Photonics* **7**, 1001 (2013).
[4] Lin, Q., Xiao, M., Yuan, L. & Fan, S. Photonic weyl point in a two-dimensional resonator lattice with a synthetic frequency dimension. *Nature Communications* **7**, 13731 (2016).
[5] Tzuang, L. D., Fang, K., Nussenzveig, P., Fan, S. & Lipson, M. Non-reciprocal phase shift induced by an effective magnetic flux for light. *Nature Photonics* **8**, 701 (2014).
[6] Fang, K. & Fan, S. Controlling the flow of light using the inhomogeneous effective gauge field that emerges from dynamic modulation. *Physical Review Letters* **111**, 203901 (2013).
[7] Kitagawa, T., Berg, E., Rudner, M. & Demler, E. Topological characterization of periodically driven quantum systems. *Physical Review B* **82**, 235114 (2010).
[8] Lindner, N. H., Refael, G. & Galitski, V. Floquet topological insulator in semiconductor quantum wells. *Nature Physics* **7**, 490 (2011).
[9] Lee, J. *et al.* Observation and differentiation of unique high-q optical resonances near zero wave vector in macroscopic photonic crystal slabs. *Physical review letters* **109**, 067401 (2012).
[10] Hsu, C. W. *et al.* Observation of trapped light within the radiation continuum. *Nature* **499**, 188 (2013).
[11] Zhao, M. & Fang, K. Mechanical bound states in the continuum for macroscopic optomechanics. *Opt. Express* **27**, 10138-10151 (2019).
[12] Fuhrmann, D. A. *et al.* Dynamic modulation of photonic crystal nanocavities using gigahertz acoustic phonons. *Nature Photonics* **5**, 605 (2011).
[13] Sohn, D. B., Kim, S. & Bahl, G. Time-reversal symmetry breaking with acoustic pumping of nanophotonic circuits. *Nature Photonics* **12**, 91 (2018).
[14] Chicone, C. *Ordinary differential equations with applications* (Springer Science & Business Media, 2006).
[15] See Supplementary Information for the calculation of Floquet bandstructure, derivation of effective gauge field, and potential experimental realizations, which includes Refs. [22-33].
[16] Haldane, F. D. M. Model for a quantum hall effect without landau levels: Condensed-matter realization of the" parity anomaly". *Physical Review Letters* **61**, 2015 (1988).
[17] Johnson, S. G. & Joannopoulos, J. D. Block-iterative frequency-domain methods for maxwells equations in a planewave basis. *Optics Express* **8**, 173–190 (2001).
[18] Rudner, M. S., Lindner, N. H., Berg, E. & Levin, M. Anomalous edge states and the bulk-edge correspondence for periodically driven two-dimensional systems. *Physical Review X* **3**, 031005 (2013).
[19] Hofstadter, D. R. Energy levels and wave functions of bloch electrons in rational and irrational magnetic fields. *Physical Review B* **14**, 2239 (1976).
[20] Lin, Q. & Fan, S. Light Guiding by Effective Gauge Field for Photons. *Physical Review X* **4**, 031031 (2014).
[21] Yanik, M. F. & Fan, S. Stopping light all optically. *Physical review letters* **92**, 083901 (2004).

[22] Combrié, S., De Rossi, A., Tran, Q. V. & Benisty, H. GaAs photonic crystal cavity with ultrahigh Q: microwatt nonlinearity at 1.55 μm. *Optics Letters* **33**, 1908–1910 (2008).

[23] Liang, H., Luo, R., He, Y., Jiang, H. & Lin, Q. High-quality lithium niobate photonic crystal nanocavities. *Optica* **4**, 1251–1258 (2017).

[24] Baba, T. Slow light in photonic crystals. *Nature Photonics* **2**, 465 (2008).

[25] Hsu, C. W. *et al.* Observation of trapped light within the radiation continuum. *Nature* **499**, 188 (2013).

[26] Jin, J. *et al.* Topologically enabled ultra-high-Q guided resonances robust to out-of-plane scattering. *arXiv:*1812.00892 (2018).

[27] Xu, C., Wang, G., Hang, Z. H., Luo, J., Chan, C. T. & Lai, Y. Design of full-k-space flat bands in photonic crystals beyond the tight-binding picture. *Scientific Reports* **5**, 18181 (2015).

[28] Notomi, M., Kuramochi, E., & Tanabe, T. Large-scale arrays of ultrahigh-Q coupled nanocavities. *Nature Photonics* **2**, 741 (2008).

[29] Balram, K. C., Davanço, M. I., Song, J. D. & Srinivasan, K. Coherent coupling between radiofrequency, optical and acoustic waves in piezo-optomechanical circuits. *Nature photonics* **10**, 346 (2016).

[30] Sohn, D. B., Kim, S. & Bahl, G. Time-reversal symmetry breaking with acoustic pumping of nanophotonic circuits. *Nature Photonics* **12**, 91 (2018).

[31] Eichenfield, M., Chan, J., Camacho, R. M., Vahala, K. J. & Painter, O. Optomechanical crystals. *Nature* **462**, 78 (2009).

[32] Fang, K. *et al.* Generalized non-reciprocity in an optomechanical circuit via synthetic magnetism and reservoir engineering. *Nature Physics* **13**, 465 (2017).

[33] Zhao, M. & Fang, K. Mechanical bound states in the continuum for macroscopic optomechanics. *Opt. Express* **27**, 10138-10151 (2019).

Acknowledgements

We are very grateful to Yu Shi and Shanhui Fan for providing the FDTD simulation code. This work is supported in part by US National Science Foundation under Grant No. ECCS-1809707.